Natural convection in a square inclined enclosure with vee-corrugated sidewalls subjected to constant flux heating from below

Salam Hadi Hussain [a], **Ahmed Kadhim Hussein** [a], **Mahmoud Moustafa Mahdi** [b]

[a] Mechanical Engineering Department
College of Engineering, Babylon University
Babylon Province, Iraq
salamphd1974@yahoo.com; ahmedkadhim74@yahoo.com

[b] Electromechanical Engineering Department
Technology University
Baghdad, Iraq
mahmoud_mahdi74@yahoo.com

Abstract. Two-dimensional steady natural convective flow in a square inclined enclosure with vertical vee-corrugated sidewalls and horizontal top and bottom surfaces has been numerically studied. A discrete heat flux strip of 24% of the total length is flush-mounted on the bottom wall, while the other non-heated parts of the bottom wall and the top wall are considered adiabatic. The two vee-corrugated sidewalls are maintained at constant cold temperature. Grashof number is varied from 10^3 to 10^6, corrugation frequency is varied from 0.5 to 2.0, corrugation amplitude has been fixed at 10% of the enclosure height and the enclosure inclination angle is varied to $0°$, $10°$, $20°$ and $30°$ respectively. The enclosure is filled with air ($Pr = 0.71$). The flow has been assumed to be steady and laminar. Fluid properties have been assumed constant except for the density change with temperature that gives rise to the buoyancy forces. The solution has been obtained using the governing equations written in terms of dimensionless variables. The dimensionless governing equations are solved using finite volume method. Results are presented in the form of streamline and isotherm plots. The results of the present work show that the natural convection phenomenon is greatly affected by increasing the enclosure inclination angle. The variation in the average Nusselt number at the bottom wall, where the heat source exists and the maximum dimensionless temperature are also presented. The results are compared and found to be in a good agreement with other published results.

Keywords: natural convection, discrete heating, vee-corrugated inclined enclosure, laminar flow, finite volume.

Nomenclature

CF	corrugation frequency	v	velocity component in y-direction (m/s)
g	gravitational acceleration (m/s^2)		
Gr	Grashof number	W	height or width of the enclosure (m)
k	thermal conductivity of fluid (W/m °C)	X	dimensionless coordinate in horizontal direction
L	heat source length (m)	x	Cartesian coordinate in horizontal direction (m)
Nu_{av}	average Nusselt number		
Nu_x	local Nusselt number	Y	dimensionless coordinate in vertical direction
P	dimensionless pressure		
p	pressure (N/m^2)	y	Cartesian coordinate in vertical direction (m)
Pr	Prandtl number		
q	heat flux per unit area (W/m^2)	α	thermal diffusivity (m^2/s)
T	temperature (°C)	β	volumetric coefficient of thermal expansion (K^{-1})
T_c	temperature of the cold surface (°C)		
U	dimensionless velocity component in x-direction	θ	dimensionless temperature
		Φ	enclosure inclination angle with horizontal direction (degree)
u	velocity component in x-direction (m/s)		
		ν	kinematic viscosity of the fluid (m^2/s)
V	dimensionless velocity component in y-direction	ρ	density of the fluid (kg/m^3)

1 Introduction

The phenomenon of natural convection heat transfer plays an important role, both in nature and in engineering systems. Many investigations have been performed on enclosures both theoretically and experimentally for a wide range of Rayleigh number (Paroncini and Corvaro [1], Raos [2] and Anilkumar and Jilani [3]). Natural convection in an air filled enclosure with vee-corrugated vertical sidewalls has received a great attention because many of the industrial applications employ this concept as a prototype. Many investigations have been carried out on heat transfer across vee-corrugated and other configured shapes. Free convection heat transfer in air layers bounded by a lower hot vee-corrugated plate and upper cold flat plate has been investigated by Elsherbiny et al. [4]. A single correlation equation in terms of Nusselt number, Rayleigh number, tilt angle and aspect ratio was developed for the aspect ratio ranging from 1 to 4 and angle of inclination ranging from 0° to 60°. They concluded that the convective heat transfer across an air layer bounded by vee-corrugated and flat plate was greater than those for parallel flat plates by a maximum of 40%.

Randall [5] considered a study of natural convection heat transfer in flat-plate and vee-corrugated enclosures. The flat plate enclosure was bounded by an isothermal, cooled surface on top and a hot surface below, while the vee-corrugated enclosure consisted of a cooled flat surface on top and a vee-corrugated heated surface below. The effects of Grashof number, tilt angle, and enclosure aspect ratio on both the local and average

heat transfer coefficients were determined for the flat plate enclosure. Grashof number range was tested from 3000 to 310000 and the aspect ratio varied between 9 and 36. The angles of tilt of the enclosure with respect to the horizontal were $45°$, $60°$, $75°$ and $90°$. Correlations were developed for both local and average Nusselt number over the range of test variables. The effect of tilt angle was found to reduce the average heat transfer by about 18 percent from the value at $45°$ to that at $90°$. No significant effect of aspect ratio over the range tested was found. Hasanuzzamana et al. [6] studied the heat transfer behavior inside the square enclosure with vee-corrugated vertical and insulated horizontal walls by changing the input power, varying the mass flow rate of water and the inlet water temperature. They found that heat transfer rate increased with the decrease of inlet water temperature. Husain and Ali [7] carried out a numerical investigation on natural convective heat transfer and fluid flow in a square cavity with vee-corrugated vertical surfaces. Their study covered the range of corrugation frequency from 1 to 3 and Grashof number from 10^3 to 10^5. The corrugation amplitude has been fixed at 5% of the enclosure height. The vorticity stream function formulation with the control volume based on finite element method has been used to study the effects of corrugation frequency and Grashof number. The results showed that the overall heat transfer through the enclosure increased with the increase in corrugation for low Grashof number; but the trend was reversed for high Grashof number. Ali and Hasanuzzaman [8] performed an experimental investigation on natural convection heat transfer through an air filled square enclosure of vee-corrugated vertical plates. They studied the variation in heat transfer rate through the square enclosure with the variation in both hot and cold plate temperatures. In their paper, hot plate temperature was varied by heat input, while the cold plate temperature was varied by considering two parameters. The first was the mass flow rate of water which was used to remove heat from cold plate and the other was the inlet temperature of water. The results showed that the increase of mass flow rate increased the heat transfer rate and the decrease in water inlet temperature increased the heat transfer rate. Saha et al. [9] studied the steady state natural convection heat transfer and fluid flow in a square enclosure with vee-corrugated vertical walls using finite element method. In their work, Grashof number was varied from 10^3 to 10^6, corrugated frequency was varied from 0.5 to 2.0 and Prandtl number was taken as 0.71. The results are presented in the form of streamline and isotherm plots. They concluded that the average Nusselt number was maximum for low corrugation frequency but the reverse trend was found for high corrugation frequency. Saha et al. [10] studied numerically a two-dimensional, steady and laminar viscous incompressible flow in a sinusoidal corrugated inclined enclosure. In their analysis, two vertical sinusoidal corrugated walls were maintained at a constant low temperature, where a constant heat flux source whose length was varied from 20 to 80% of the total length of the enclosure was discretely embedded at the bottom wall. The penalty finite element method has been used to solve the governing Navier–Stokes and energy conservation equations of the fluid medium in the enclosure in order to investigate the effects of inclination angles and discrete heat source sizes on heat transfer for different values of Grashof number. Results are presented in the form of streamline and isotherm plots. It was concluded that the average Nusselt number increased as inclination angle increased for different heat source sizes. On the other hand, natural convection

problem in differentially heated square enclosures has been studied extensively. Sharif and Mohammad [11] studied numerically natural convection in rectangular cavities using a finite volume method. Their study was based on a configuration, where a constant flux heat source was symmetrically embedded at the bottom wall. The length of the heat source was varied from 20 to 80% of the total length of the bottom wall. The non-heated parts of the bottom wall were considered adiabatic. The Grashof number was varied from 10^3 to 10^6, aspect ratios ranging from 0.5 to 2 and inclination angles of the cavity from $0°$ to $30°$. Results are presented in the form of streamline and isotherm plots as well as the variation of the Nusselt number and maximum temperature at the heat source surface under different conditions. Al-Bahi et al. [12] studied numerically the effect of inclination angle on the steady laminar free convection in a rectangular enclosure, which was discretely heated by an isoflux flush mounted small heater. The effect of the orientation angle on the flow structure and associated transition between unicellular and multiple cell flow was presented. The maximum Nusselt number was found close to the vertical orientation while the minimum was at the horizontal position with fluid heated from the top for which convection was effectual and the average Nusselt number was greater than unity. Saha et al. [13] studied numerically natural convection in a two-dimensional rectangular enclosure using a finite element method. In their work, top wall was considered adiabatic, two vertical walls were maintained at constant low temperature, the bottom wall was maintained at constant high temperature and the non-heated parts of the bottom wall are considered adiabatic. Grashof number was varied from 10^3 to 10^6, aspect ratios ranging from 0.5 to 1, inclination angles of the enclosure from $0°$ to $30°$ and Prandtl number was taken as 0.71. Results are presented in the form of streamline and isotherm plots as well as the variation in the Nusselt number at the heat source surface under different conditions. From the above literature review, it is noticed that there are some restricted studies on vee-corrugated inclined enclosure. The major object of the present work is to investigate the effect of the inclination angle on the heat transfer and fluid flow for natural convection in a vee-corrugated inclined enclosure. The present work develops the work of Saha et al. [9] by studying the effect of enclosure inclination angle on the natural convection in a square inclined enclosure with vee-corrugated sidewalls subjected to constant flux heating from below. This important modification point is not studied in the work of Saha et al. [9].

2 Problem description and the mathematical analysis

A sketches of the two-dimensional vee-corrugated inclined square enclosure of dimensions ($W \times W$) are shown in Figs. 1 and 2 respectively. It consists of two inclined vee-corrugated sidewalls at constant temperature T_c. The present model is based on the geometry of work of Saha et al. [9], where a discrete heat flux strip of 24% of the total length L is flush-mounted to the bottom wall, while the other non-heated parts of the bottom wall and the top wall are considered adiabatic. Grashof number was varied from 10^3 to 10^6, corrugation frequency was varied from 0.5 to 2.0, corrugation amplitude has been fixed at 10% of the enclosure height and the enclosure inclination

angle Φ, was varied to be $\Phi = 0°$, $10°$, $20°$ and $30°$. The enclosure is filled with air ($Pr = 0.71$) which is considered Newtonian and incompressible while viscous dissipation effects are considered negligible with constant properties except for the density in the buoyancy force. The Boussinesq approximation is used to relate the variable density to the local temperature. The flow inside the enclosure is assumed laminar and steady. The main purpose of the present work is to study the effect of enclosure inclination angle on the natural convection in a square enclosure with vee-corrugated sidewalls subjected to constant flux heating from below.
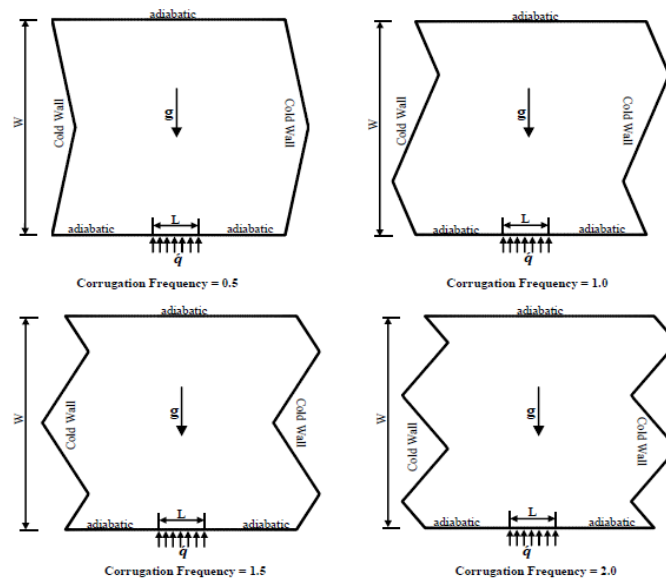

Fig. 1. Schematic diagram of the calculation domain at an inclination angle $\Phi = 0°$.

2.1 Governing equations

The dimensionless steady-state equations for mass, momentum and energy in the Cartesian coordinates (X, Y) are given as follows:

$$\frac{\partial U}{\partial X} + \frac{\partial V}{\partial Y} = 0, \tag{1}$$

$$U\frac{\partial U}{\partial X} + V\frac{\partial U}{\partial Y} = -\frac{\partial P}{\partial X} + \left(\frac{\partial^2 U}{\partial X^2} + \frac{\partial^2 U}{\partial Y^2}\right) + Gr\theta\sin\Phi, \tag{2}$$

$$U\frac{\partial V}{\partial X} + V\frac{\partial V}{\partial Y} = -\frac{\partial P}{\partial Y} + \left(\frac{\partial^2 V}{\partial X^2} + \frac{\partial^2 V}{\partial Y^2}\right) + Gr\theta\cos\Phi, \tag{3}$$

$$U\frac{\partial\theta}{\partial X} + V\frac{\partial\theta}{\partial Y} = \frac{1}{Pr}\left(\frac{\partial^2\theta}{\partial X^2} + \frac{\partial^2\theta}{\partial Y^2}\right), \tag{4}$$

where

$$\theta = \frac{T - T_c}{\Delta t}, \quad X = \frac{x}{W}, \quad Y = \frac{y}{W}, \quad U = \frac{uL}{\nu}, \quad V = \frac{vL}{\nu},$$

$$\Delta t = \frac{qW}{k}, \quad P = \frac{pL^2}{\rho \nu^2}, \quad Pr = \frac{\nu}{\alpha} \quad \text{and} \quad Gr = \frac{g\beta \Delta t W^3}{v^2}.$$

2.2 Boundary conditions

The boundary conditions which are used in the present work can be specified as follows:

$$U = V = 0 \text{ (all walls)}, \quad \frac{\partial \theta}{\partial Y} = 0 \text{ (top wall)}, \quad \theta = 0 \text{ (right and left walls)},$$

$$\frac{\partial \theta}{\partial Y} = \begin{cases} 0 & \text{for } 0 < X < 0.48, \\ -1 & \text{for } 0.48 \leq X \leq 0.62, \quad \text{(bottom wall)}. \\ 0 & \text{for } 0.62 < X < 1.2 \end{cases}$$

2.3 Local and average Nusselt numbers

The rate of heat transfer is computed at each wall and is expressed in terms of local surface Nusselt number (Nu_x) and surface-averaged Nusselt number (Nu_{av}) as given by Saha et al. [9]:

$$Nu_x = \frac{1}{\theta_X(X)}, \tag{5}$$

$$Nu_{av} = \frac{W}{L} \int_0^{L/W} \frac{1}{\theta_X(X)} \, dX, \tag{6}$$

where $\theta_X(X)$ is the dimensionless local temperature.

3 Solution procedure

The preferred method for the present numerical simulation is the two-dimensional finite volume method of Patankar [14]. In this investigation, a non-uniformly collocated grid procedure is used in primitive variables with a power-law differencing scheme for the convection terms, whereas a central differencing is used to discretize the diffusion terms. The steady state governing equations (1)–(4) are solved by the finite volume method using Patankar's algorithm (Patankar [14]). The finite volume method is a method of discretization in space of the entire domain, which can use a mesh with finite number of volumes (Barth and Ohlberger [15]).The enclosure is divided with non-uniform and non-orthogonal grid on the sub-volumes. Each of control volume surrounds one nodal point in its center called discretization point. In the numerical scheme used in the present work, it is necessary to link the pressure and velocity so the numerical algorithm that can

solve all variables with velocity and pressure linked equation. The solution procedure starts with input data and initial values. Velocities, temperatures and pressures are calculated by solving algebraic equations. After than the Nusselt number is calculated. If a convergence criterion is obtained, the output file is printed. Otherwise, it goes to starting point. Schematic of grid arrangement is given in Fig. 2 and the discretization process is performed according to this grid arrangement. This methodology is a interactive process, where the error or residual is compared to a reference error, also named "target error". In this way, flow and heat transfer simulations require the introduction of suitable flow and heat transfer models to guarantee a satisfactory convergence. The calculation process stops when the maximum difference between two consecutive field values of variables is less than or equal to 10^{-6}.
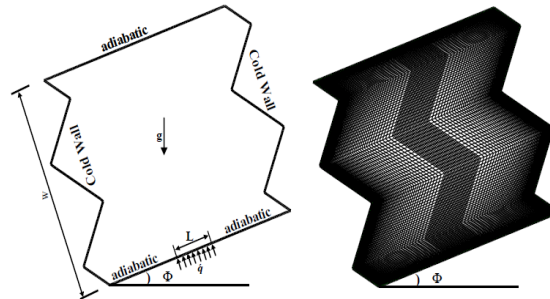

Fig. 2. Schematic physical configuration and boundary conditions (left) and a typical grid distribution (120×120) with non-uniform and non-orthogonal distributions (right) for inclined vee-corrugation square enclosure at corrugation frequency $CF = 2.0$.

4 Grid sensitivity test

The numerical scheme used to solve the governing equations for the present work is a finite volume approach. It provides smooth solutions at the interior domain including the corners. The enclosure is meshed with a non-uniform rectangular grid with a very fine spacing near the walls. As shown in Fig. 2, the 2-D computational grids are clustered towards the walls. The location of the nodes is calculated using a stretching function so that the node density is higher near the walls of the enclosure. Solutions are assumed to converge when the following convergence criterion is satisfied at every point in the solution domain:

$$\left| (\Phi_{new} - \Phi_{old}) / \Phi_{old} \right| \leq 10^{-6}, \tag{7}$$

where Φ represents primary variables U, V, P and θ. In order to obtain grid independent solution, a grid refinement study is performed for $Gr = 10^4$ and 10^6, $Pr = 0.71$, $CF = 0$ and 2.0, and $\Phi = 0°$. In the present work, nine combinations (80×80, 90×90, 95×95, 100×100, 120×120, 150×150, 175×175, 200×200 and 225×225) of control volumes are used to test the effect of grid size on the accuracy of the predicted results. Figs. 3(a) and 3(b) show the convergence of the average Nusselt number Nu_{av}, at the constant heat flux surface with grid refinement. It is observed that grid independence is achieved

with combination of (120×120) control volumes, where there is insignificant change in Nu_{av} with the improvement of finer grid. The agreement is found to be excellent which validates the present computations indirectly.
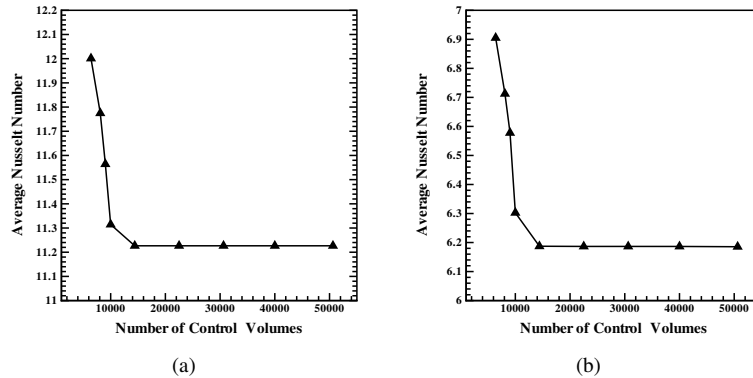

Fig. 3. Convergence of average Nusselt number along the constant heat flux middle bottom wall with grid refinement for (a) $Gr = 10^4$, $Pr = 0.71$, $CF = 0$ and $\Phi = 0°$; (b) $Gr = 10^6$, $Pr = 0.71$, $CF = 2.0$ and $\Phi = 0°$.

5 Numerical results verification

The present numerical approach is verified against the results published by Saha et al. [9] for natural convection heat transfer in square enclosure with vee-corrugated vertical walls ($CF = 0.5$) for different Grashof numbers, Gr as shown in Table 1 and 2 respectively. The comparison is made using the following parameters: $Pr = 0.71$, $Gr = 10^3$ to 10^6 and $\Phi = 0°$. The normalized length of the constant flux heat source at the bottom wall is fixed at $L/W = 0.2$. It is seen in this comparison that both average Nusselt numbers at the heated surface and maximum surface temperature are in good agreement with a maximum deviation of about 1.240%. This validation makes a good confidence in the present numerical model to deal with the same square enclosure configuration problem (except the normalized length of the constant flux heat source at the bottom wall was fixed at $L/W = 0.24$ instead of $L/W = 0.2$) but it is considered inclined with different angles of inclination ($\Phi = 10°$, $20°$ and $30°$) to calculate the flow and thermal fields in the present work.

Table 1. Comparison of present surface-averaged Nusselt number with those of previous numerical study for validation at $CF = 0.5$, $\Phi = 0°$, $L/W = 0.2$ and $Pr = 0.71$.

Gr	Mean Nusselt number at the heated bottom wall		
	Present study	Saha et al. [9]	Error (%)
10^3	6.022212	6.012256	0.165
10^4	6.053254	6.052548	0.0116
10^5	7.428247	7.435621	-0.100
10^6	11.497665	11.57548	-0.672

Table 2. Comparison of present maximum temperature with those of previous numerical
study for validation at $CF = 0.5$, $\Phi = 0°$, $L/W = 0.2$ and $Pr = 0.71$.

	Mean Nusselt number at the heated bottom wall		
Gr	Present study	Saha et al. [9]	Error (%)
10^3	0.180612	0.1805112	0.055
10^4	0.180522	0.1805114	0.005
10^5	0.156058	0.154205	1.201
10^6	0.108786	0.1074528	1.240

6   Results and discussion

The properties of the temperature and flow fields in a square inclined enclosure with
vertical vee-corrugated sidewalls and horizontal top and bottom surfaces are examined
and discussed in this section. The following ranges of the dimensionless parameters
are considered: The Prandtl number $Pr = 0.71$, Grashof number is varied from 10^3
to 10^6, the normalized length of the constant flux heat source at the bottom wall was
fixed at $L/W = 0.24$, corrugation frequency is varied from 0.5 to 2.0 and the enclosure
inclination angle is varied to $0°$, $10°$, $20°$ and $30°$. Figs. 4, 5, 6 and 7 present the
isotherms and streamlines for Grashof number from 10^3 to 10^6 at different inclination
angles and various corrugation frequency using flow conditions ($Pr = 0.71$, $L/W =
0.24$) respectively. In all these figures, when the inclination angle is zero, the flow field
begins to grow along the vertical mid plane and then stops near the adiabatic top wall.
After this, the top wall causes the flow field to turn horizontally towards the isothermal
cold sidewalls and then moves downwards along the isothermal cold sidewalls and turns
back horizontally to the central region after hitting the bottom wall. Similar behaviour
is noticed in results of Saha et al. [9] which validates the present computations process.
Furthermore, the isotherm contours are also symmetrical about the vertical symmetry
axis and collects morly near the hot bottom wall, where the heat source exists. These
isotherms show that a large temperature gradient exists there. Again similar behaviour
can be noticed in work of Saha et al. [9]. When the enclosure inclination angle is zero
and the range of Grashof numbers are low (as shown in Figs. 4 and 5 respectively), the
buoyancy force effect is small, so for this case the convection heat transfer contribution
is small and the diffusion heat transfer is dominant because the generated buoyancy
force is not strong enough to initiate fluid convection. When Grashof number range
increases (as shown in Figs. 6 and 7), the buoyancy force effect becomes larger so the
vortices shape becomes irregular due to the effective fluid motion coming from the higher
temperatures near the bottom wall, where the heat source exists and as a result making a
large convection heat transfer contribution. On the other hand, in all these figures it can
be observed that the isotherm lines shape changes significantly from the uniform, almost
linear and symmetrical shape at the upper part of the enclosure (as shown in Figs. 4 and 5
respectively), to non-symmetry, uniform horizontal and linear vertical shape at the upper
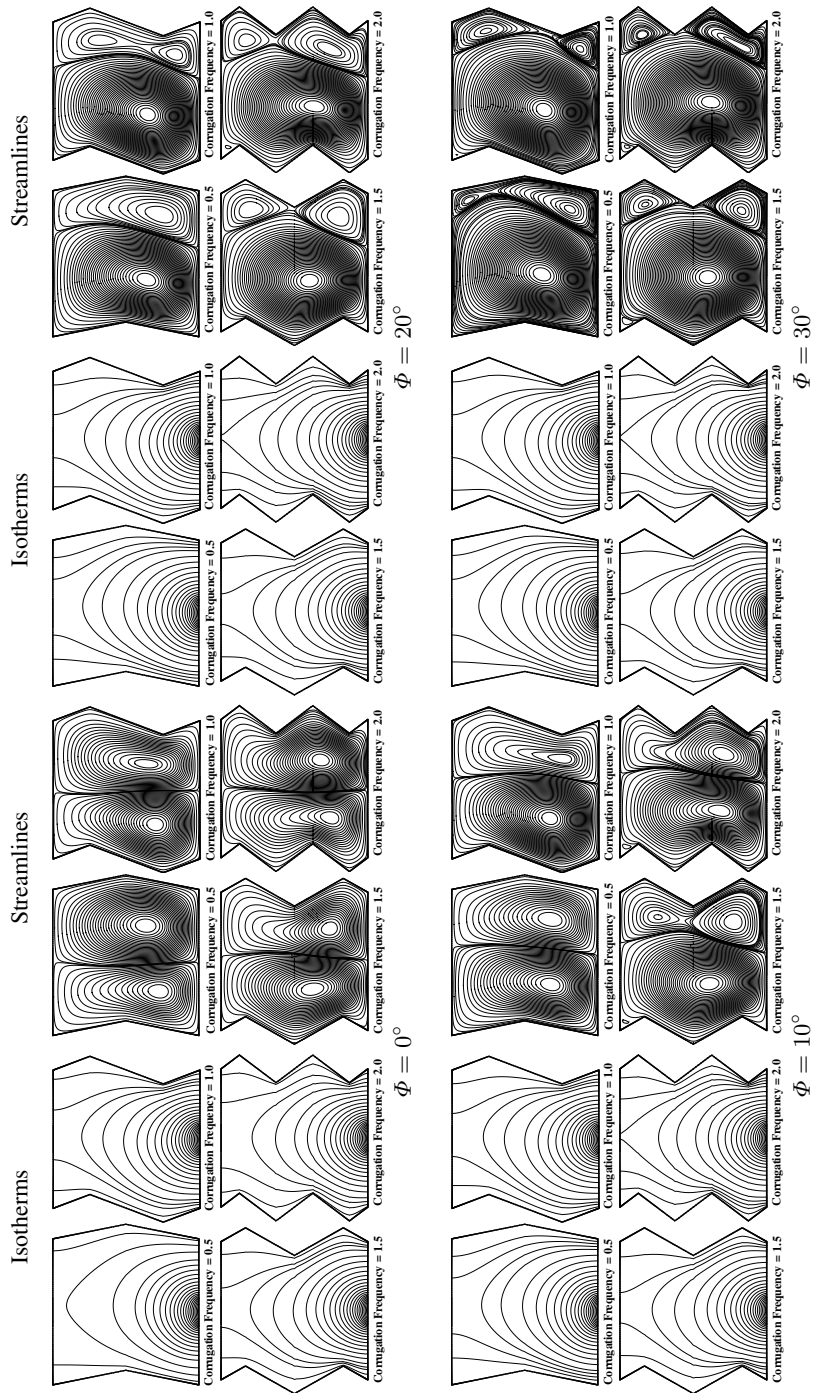part of the enclosure (as shown in Figs. 6 and 7 respectively).

Fig. 4. Isotherms and streamlines for Grashof number, $Gr = 10^3$ at different inclination angles using the flow conditions ($Pr = 0.71$, $L/W = 0.24$).
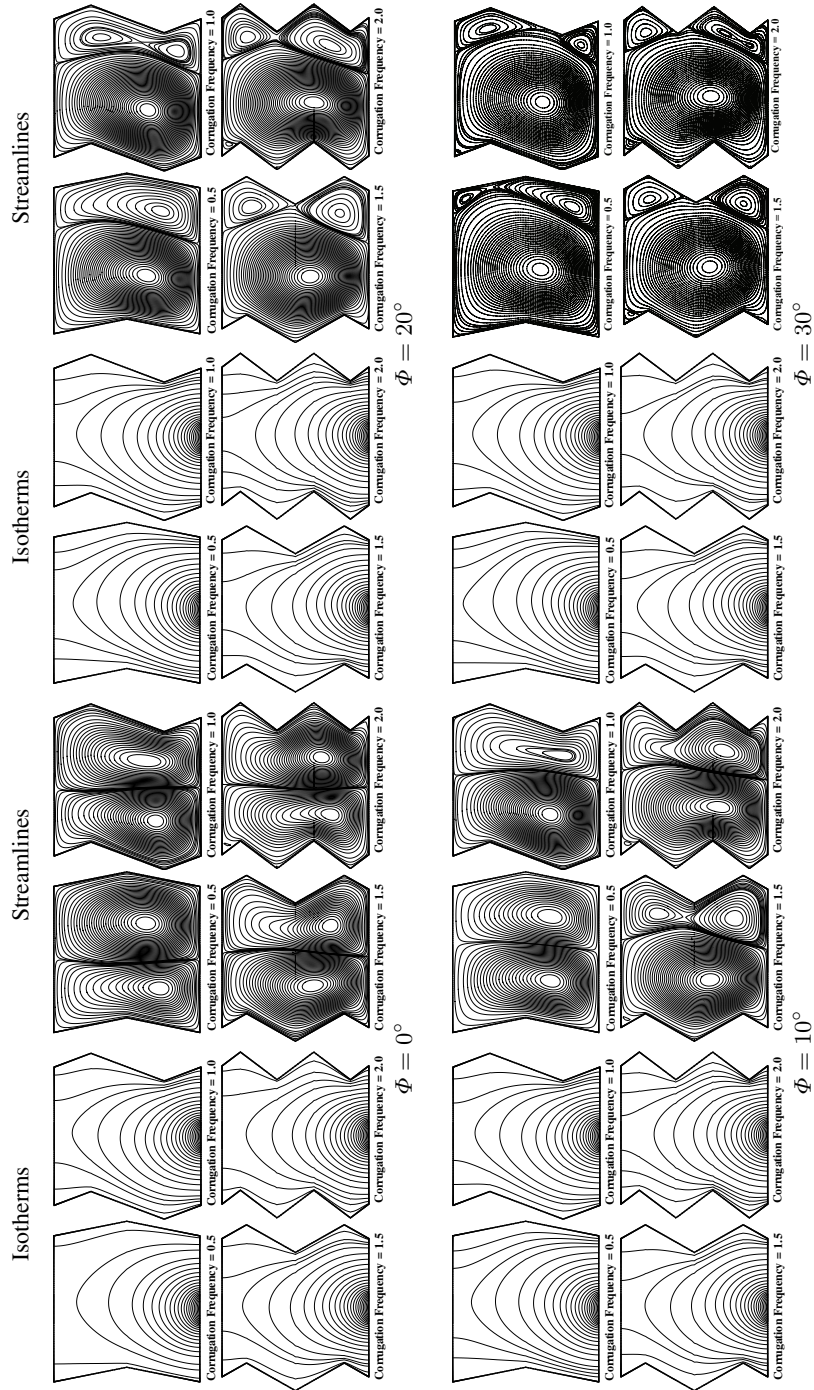
Fig. 5. Isotherms and streamlines for Grashof number, $Gr = 10^4$ at different inclination angles using the flow conditions ($Pr = 0.71$, $L/W = 0.24$).
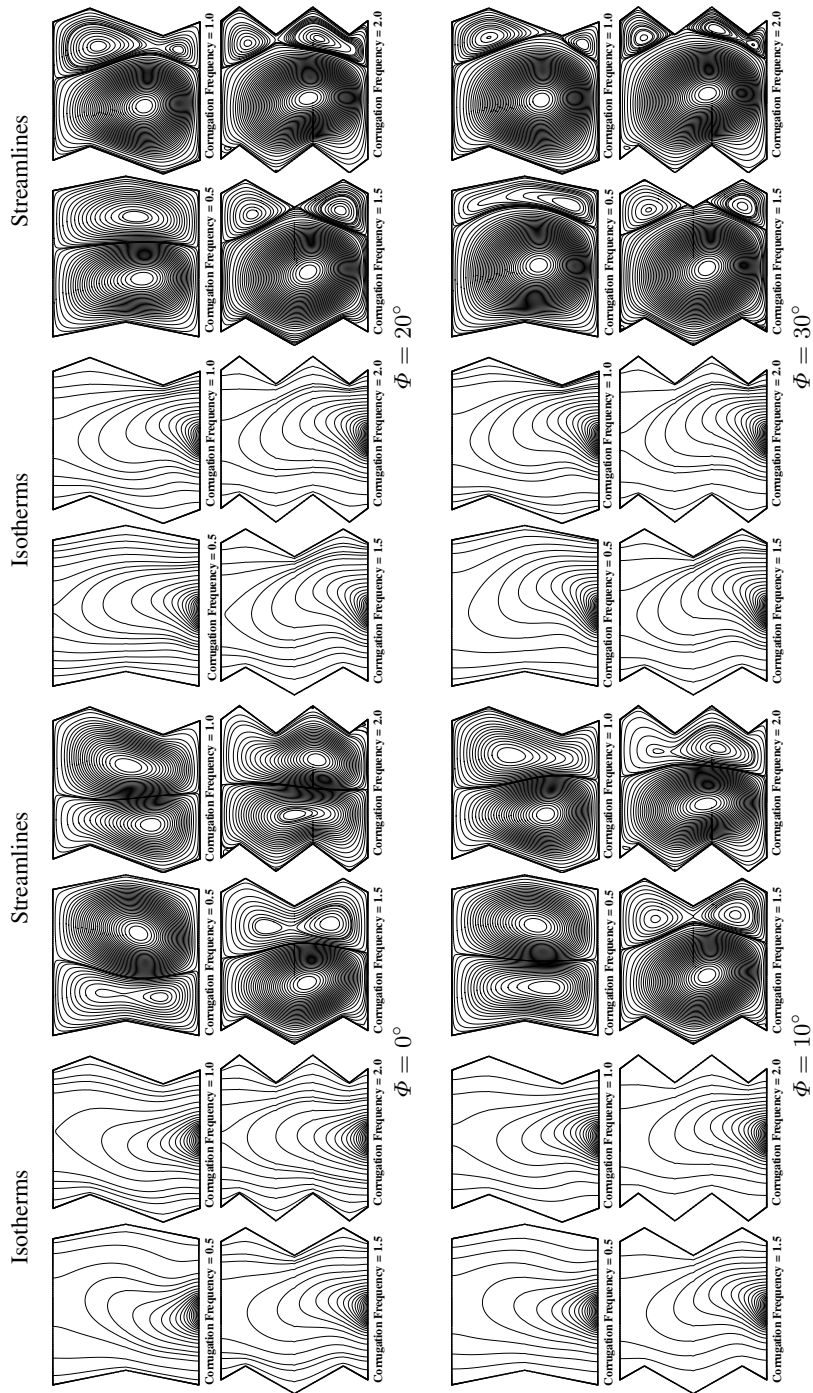
Fig. 6. Isotherms and streamlines for Grashof number, $Gr = 10^5$ at different inclination angles using the flow conditions ($Pr = 0.71$, $L/W = 0.24$).
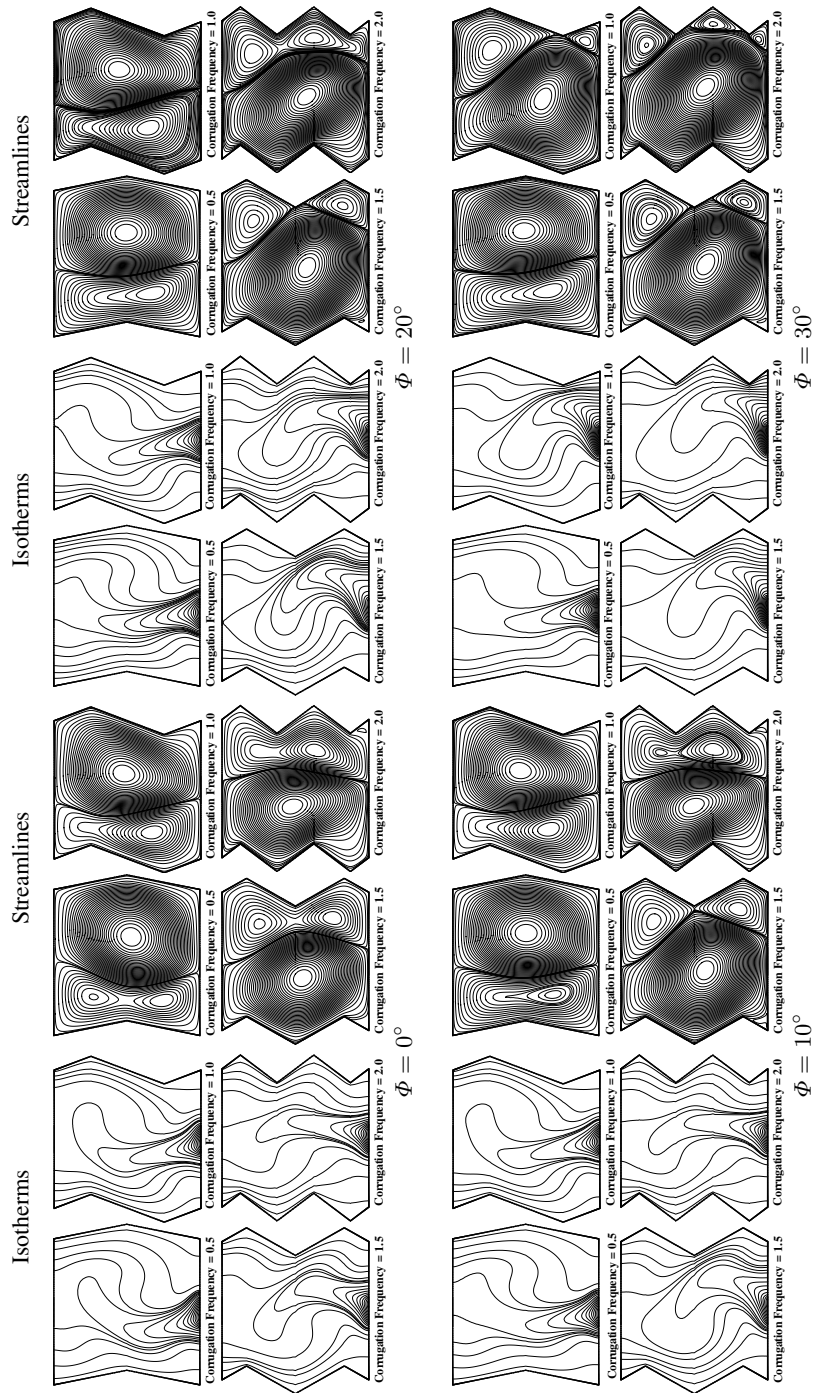
Fig. 7. Isotherms and streamlines for Grashof number, $Gr = 10^6$ at different inclination angles using the flow conditions ($Pr = 0.71$, $L/W = 0.24$).

The results show also that the thermal boundary layers near the bottom wall, where the heat source exists increase and concentrate as Grashof number increases. Now, when the enclosure inclination angle increases to 10°, 20° and 30° and Grashof number is low (as shown in Figs. 4 and 5 respectively), the effect of inclination angle on the streamlines and isotherms contour is weak but when Grashof number increases (as shown in Figs. 6 and 7 respectively) the flow and thermal fields have a different nature. The reason for this nature, is that the buoyancy force effect resulting from the heat source at the bottom wall is small when the effect of inclination angle is small, while the effect of buoyancy force which becomes more dominant, as the inclination angle increases causes a clear irregularity in the vortices shape due to the flow confusion which causes a clear convection heat transfer effect. Also, the thermal boundary layers near the bottom wall increase and concentrate as the inclination angle and Grashof number increase. The reason for this phenomenon is that the fluid internal motion near the hot inclined bottom wall is more dominant than that near the cold right and left sidewalls.
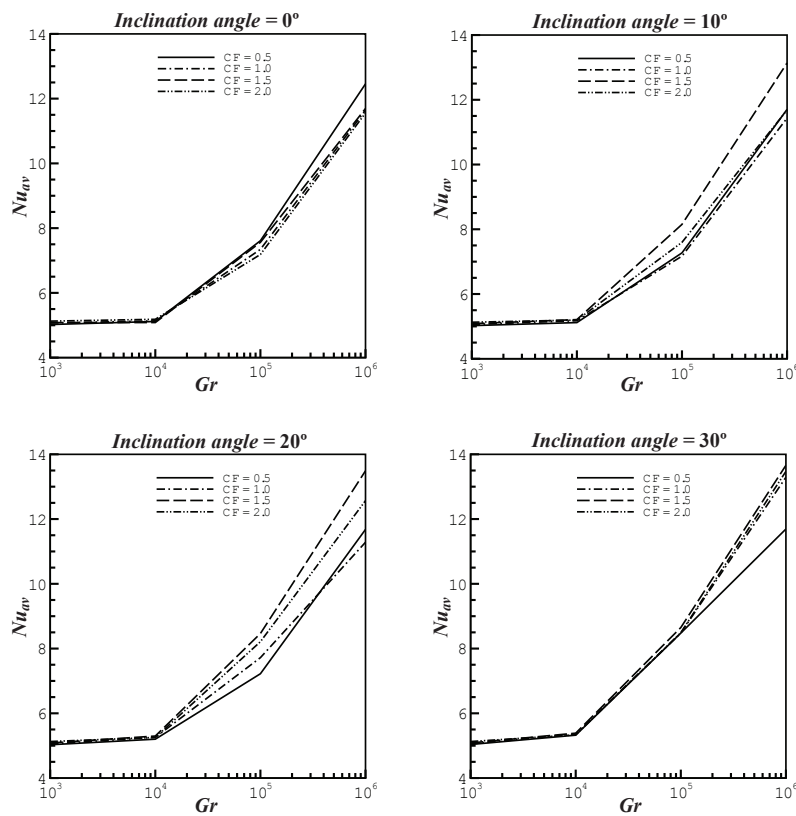

Fig. 8. Comparison of the average Nusselt number Nu_{av} at the constant flux heated bottom surface for various Grashof numbers and corrugation frequencies with different inclination angles.

The variation in the average Nusselt number at the bottom wall, where the heat source exists for various Grashof numbers and corrugation frequencies with different inclination angles is explained in Fig. 8. From this figure, it is noticed that the average Nusselt number increases dramatically with Grashof number and inclination angles at any particular corrugation frequencies. This is due to the increase in the intensity of convection currents which causes a clear change in the heat transfer rate especially for Grashof number greater than 10^4 with different inclination angles. When Grashof number is less than or equal to 10^4, the average Nusselt number almost has a constant behaviour with the increase in inclination angles, since the buoyancy force effect is weak, so the convection heat transfer contribution is weak also, and the diffusion heat transfer is dominant.

The variation in the maximum dimensionless temperature at the bottom wall, where the heat source exists for various Grashof numbers and corrugation frequencies with different inclination angles is explained in Fig. 9.
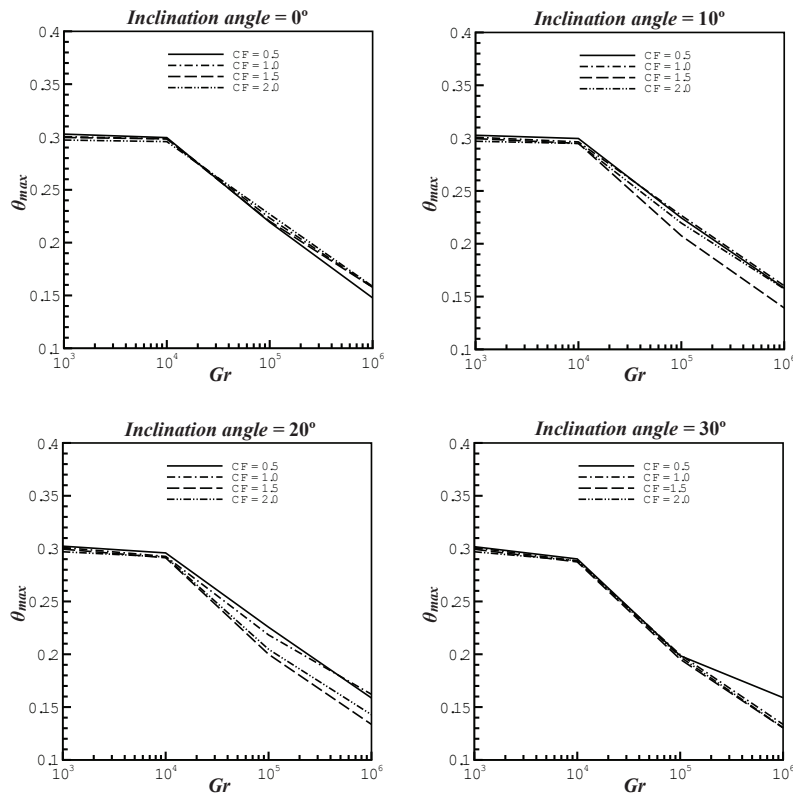

Fig. 9. Comparison of the maximum temperature θ_{max} for various Grashof numbers and corrugation frequencies with different inclination angles.

From this figure, it is observed that the maximum dimensionless temperature decreases significantly for Grashof number greater than 10^4 with different inclination an-

gles. When Grashof number is less than or equal to 10^4, the maximum dimensionless temperature is almost invariant with the increase in inclination angles.

7 Conclusions

The following conclusions can be drawn from the results of the present work:

1. When the inclination angle is zero; the flow field begins to grow along the vertical mid plane and then stops near the adiabatic top wall. On the other hand, the isotherm contours are also symmetrical about the vertical symmetrical axis and collects near the hot bottom wall, where the heat source exists and a large temperature gradient can be observed there.

2. When the enclosure inclination angle is zero and the range of Grashof numbers is low (10^3 and 10^4), the buoyancy force effect is small and the convection intensity is weak. When the Grashof number range increases (10^5 and 10^6), the buoyancy force effect becomes larger so the convection intensity becomes high and strong.

3. The flow field is characterized by recirculating vortices which fill most size of the enclosure. The results show also that the thermal boundary layers near the bottom wall increase and concentrate as Grashof number increases.

4. When the enclosure inclination angle increases as $10°$, $20°$ and $30°$ respectively and the Grashof number is low, the effect of inclination angle on the streamlines and isotherms contours is weak. But when the Grashof number increases the flow and thermal fields have a clear nature as the enclosure inclination angle increases.

5. When the inclination angle and Grashof number increase, the thermal boundary layers increase and concentrate near the bottom wall, whereg the heat source exists.

6. For Grashof number greater than 10^4 in different inclination angles, the average Nusselt number increases at any particular corrugation frequencies. But when Grashof number is less than or equal to 10^4, the average Nusselt number is almost invariant with the increase in inclination angles.

7. For Grashof number greater than 10^4 in different inclination angles, the maximum dimensionless temperature decreases at any particular corrugation frequencies. But when Grashof number is less than or equal to 10^4, the maximum dimensionless temperature almost has a constant behaviour with the increase in inclination angles.

and recommendations to improve our work. Furthermore, the authors would like to thank the editor for this follow-up to maintain the quality of the published papers in the journal "Nonlinear Analysis: Modelling and Control".

References

1. O. Aydin, W. Yang, Natural convection in enclosures with localized heating from below and symmetrical cooling from sides, *Int. J. Numer. Methods Heat Fluid Flow*, **10**(5), pp. 518–529, 2000.

2. M. Raos, Numerical investigation of laminer natural convection in inclined square enclosures, *Facta Univ., Ser. Phys. Chem. Technol.*, **2**(3), pp. 149–157, 2001.

3. S.H. Anilkumar, G. Jilani, Convective heat transfer enhancement in an enclosure with fin utilizing nano fluids, International Journal of Mechanical, Industrial and Aerospace Engineering, **3**(2), pp. 104–111, 2009.

4. S.M. Elsherbiny, K. Holland, G. Daithby, Free convection across inclined air layers with one surface V-corrugated, in: *Heat Transfer Solar Energy Systems*, ASME, New York, pp. 432–438, 1977.

5. R.K. Randall, An interferometric study of natural convection heat transfer in flat-plate and vee-corrugated enclosures, Ph.D. Thesis, Wisconsin Univ., Madison, 1978.

6. R.K. Randall, Interferometer investigation of convection in salt-flat plate and V-corrugated solar collectors, *J. Heat Trans., Trans. ASME*, **101**, pp. 120–125, 1979.

7. S. Husain, M. Ali, Effect of corrugation frequencies on natural convective heat transfer and flow characteristics in a square enclosure of vee-corrugated vertical walls, *Int. J. Energ. Res.*, **17**(8), pp. 697–708, 1993.

8. M. Ali, M. Hasanuzzaman, Heat transfer by natural convection through V-corrugated plates, Journal of Mechanical Engineering, **36**, pp. 1–5, 2006.

9. G. Saha, S. Saha, M. Ali, M.Q. Islam, Natural convection in a vee-corrugated square enclosure with discrete heating from below, *J. Eng. Technol.*, **6**(1), pp. 15–27, 2007.

10. S. Saha, T. Sultana, G. Saha, M. Rahman, Effects of discrete isoflux heat source size and angle of inclination on natural convection heat transfer flow inside a sinusoidal corrugated enclosure, *International Communications in Heat and Mass Transfer*, **35**(10), pp. 1288–1296, 2008.

11. M. Sharif and T. Mohammad, Natural convection in cavities with constant flux heating at the bottom wall and isothermal cooling from the sidewalls, *Int. J. Therm. Sci.*, **44**, pp. 865–878, 2005.

12. A. Al-Bahi, M. Hazmy and G. Zaki, Natural convection in a tilted rectangular enclosure with a single discrete heater, *KAU Journal of Engineering Sciences*, **16**(2), pp. 141–167, 2006.

13. G. Saha, S. Saha, M. Quamrul Islam, M.A. Razzaq Akhanda, Natural convection in enclosure with discrete isothermal heating from below, *Journal of Naval Architecture and Marine Engineering*, **4**, pp. 1–13, 2007.

14. S. Patankar, *Numerical Heat Transfer and Fluid Flow*, Hemisphere Publishing Corporation, New York, 1980.

15. T. Barth, M. Ohlberger, Finite volume methods: foundation and analysis, in: E. Stein, R. de Borst, T.J.R. Hughes (Eds.), *Encyclopedia of Computational Mechanics*, Vol. 1, John Wiley & Sons Ltd., 2004.